Supplemental Data. Leplé et al. (2007). Down-regulation of cinnamoyl-coenzyme A reductase in poplar (*Populus tremula* x *P. alba*); multiple level phenotyping reveals effects on cell wall polymer metabolism and structure.

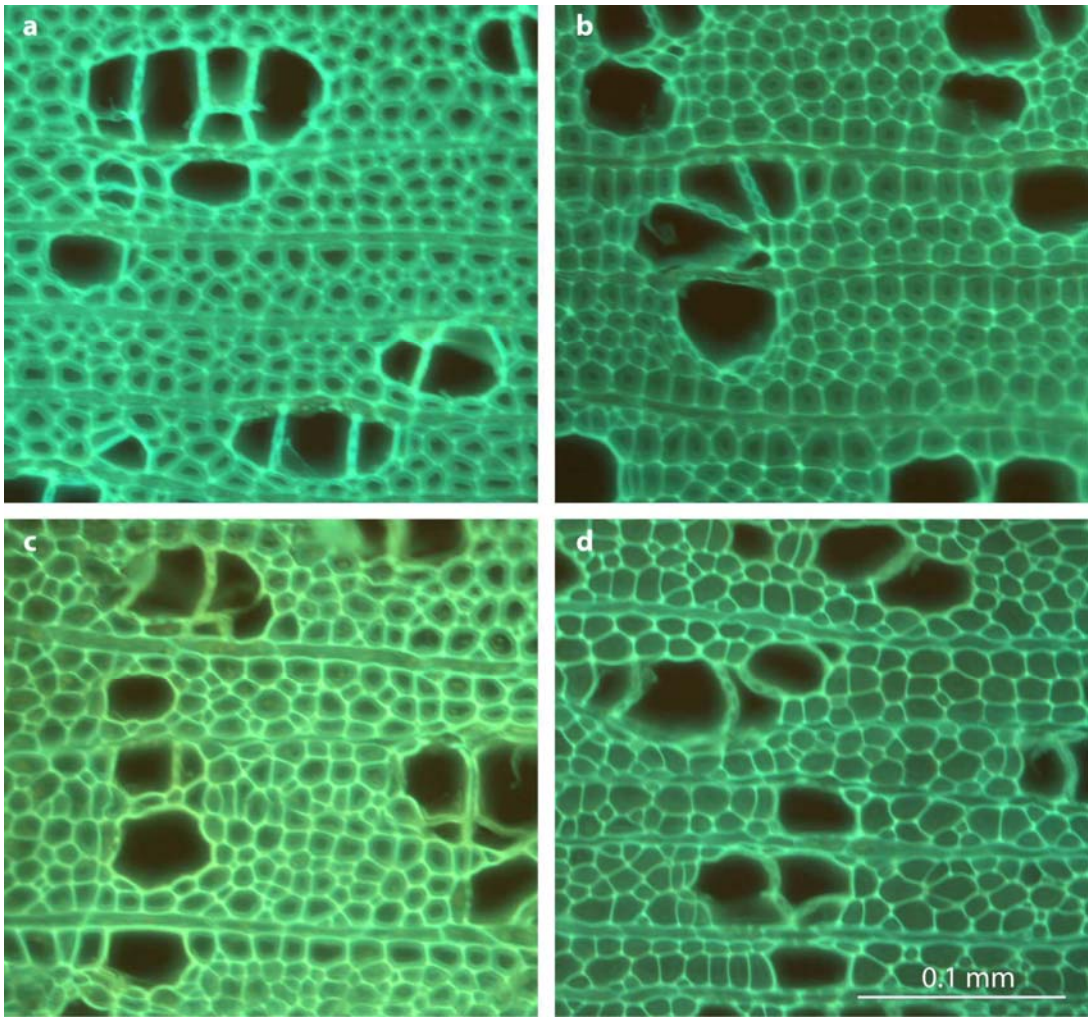

Supplemental Figure 1. Long wavelength UV-excited autofluorescence.

Long wavelength UV-excited autofluorescence (excitation wavelength 355-425 nm and longwave pass filter at 470 nm) of stem sections of a 6-month-old greenhouse-grown *CCR*-down-regulated poplar (FAS13) with patchy orange-brown xylem coloration; whitish xylem area (a-b); orange-brown area (c-d). b and d: after alkali treatment (NaOH 5 N, 2 min). The autofluorescence in the whitish areas of the transformants is blue-green (a), reminiscent to WT (not shown), whereas it is yellow-green in the orange-brown areas, with the strongest intensity in the vessels (c). After alkali treatment, the autofluorescence in the orange-brown areas becomes blue-green (d), similar to the autofluorescence in non-discolored xylem of the transformant (b) and in WT (not shown); viewed at pH 10.3.

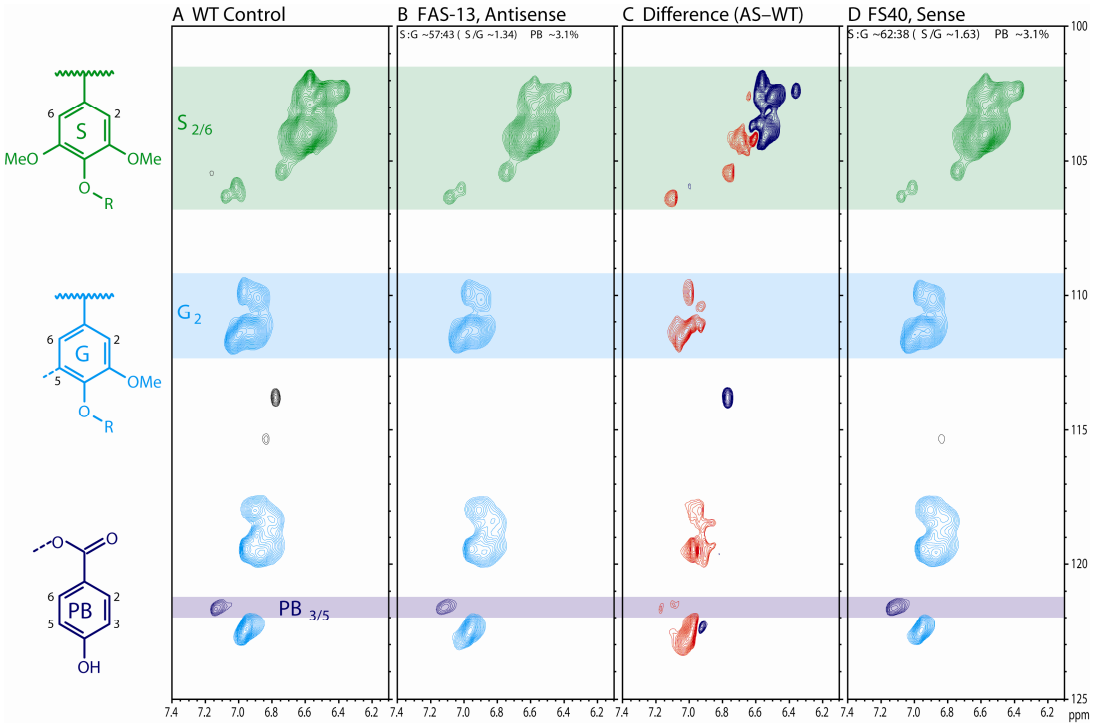

Supplemental Figure 2. Aromatic regions of HSQC spectra from milled-wood extracted lignins illustrating compositional changes.

Lignins isolated from **(A)** the wild-type control, **(B)** the FAS13 antisense-*CCR* line, **(C)** the difference spectrum (FAS13 – WT) showing the decreased S levels (negative, blue), increased (relative) G levels (positive, red), and minor increase in *p*-hydroxybenzoates, PB. **(D)** The FS40 sense *CCR* line.

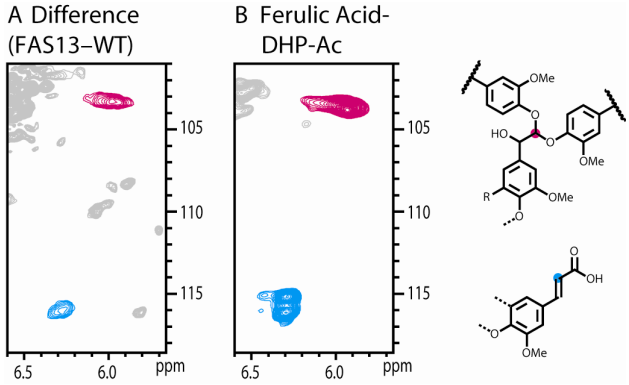

Supplemental Figure 3. Partial HSQC NMR spectra providing evidence for ferulic acid incorporation into lignins.

(A) A two-dimensional difference spectrum from lignins isolated from the FAS13 minus the WT showing the ferulate *bis*-8–O–4-ether structure (magenta, the 8-C/H-correlation at ~104/6.0 ppm, detectable in the transgenic but not in WT) from which the thioacidolysis marker derives, and the 4–O-etherified (ring-attached) ferulic acid (cyan, 116/6.3 ppm).

(B) Same region from the spectrum of a synthetic lignin (DHP) derived from 50:50 sinapyl:coniferyl alcohol and incorporating ~5% 8-^{13}C-labeled ferulic acid. The analogous contours are colored.

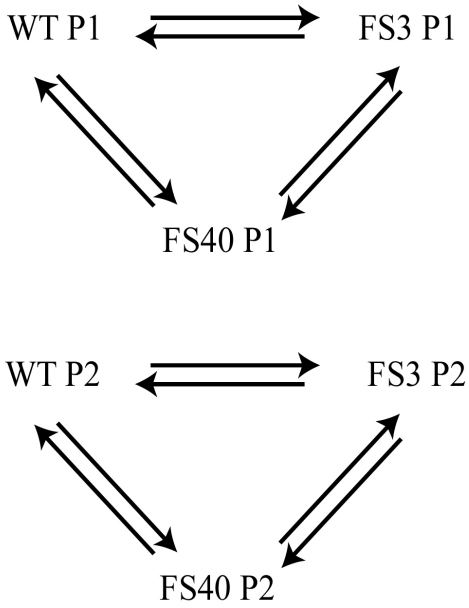

Supplemental Figure 4. Experimental setup of microarray analyses: all pairwise comparison design

Pool 1 of WT cDNA was hybridized to the microarrays together with pool 1 of FS3 cDNA and together with pool 1 of FS40 cDNA. In addition, pool 1 of FS3 cDNA was hybridized to the microarrays together with pool 1 of FS40 cDNA. All hybridizations were done with a dye-swap replication, as indicated by the double arrows, thus, providing a technical replication. The same experimental setup was followed using the second pool of cDNA of each line. WT, wild type; P1, pool 1; P2, pool 2.

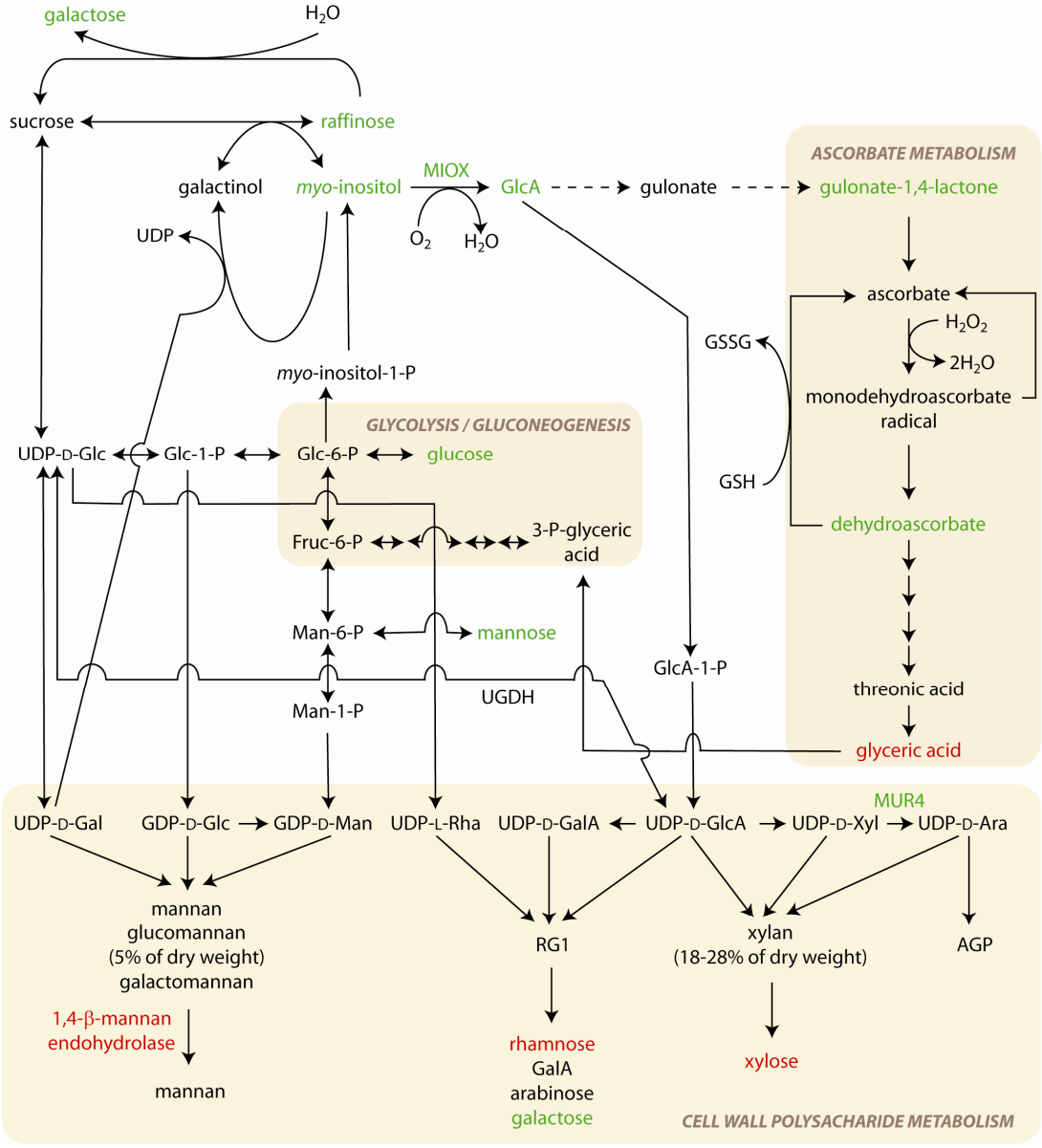

Supplemental Figure 5. Differentially accumulating transcripts and metabolites of general carbohydrate, ascorbate, hemicellulose, and pectin metabolism.

Metabolites whose accumulation was decreased and enzymes whose corresponding transcript levels were decreased in the *CCR*-down-regulated transgenic poplar lines as compared to the WT levels, are indicated in green. Metabolites of which the accumulation was increased and enzymes of which the corresponding transcript levels were increased in the *CCR*-down-regulated transgenic poplar lines, are indicated in red. Dashed arrows indicate enzymatic reactions that have not been demonstrated in plants. Ara, arabinose; Fruc, fructose; Gal, galactose; Glc, glucose; GlcA, glucuronate; Man, mannose; Rha,

rhamnose; Xyl, xylose; RGI, rhamnogalacturonan type I; AGP, arabinogalactan protein; -P, -phosphate; MIOX, *myo*-inositol oxygenase; UGDH, UDP-D-glucose dehydrogenase.

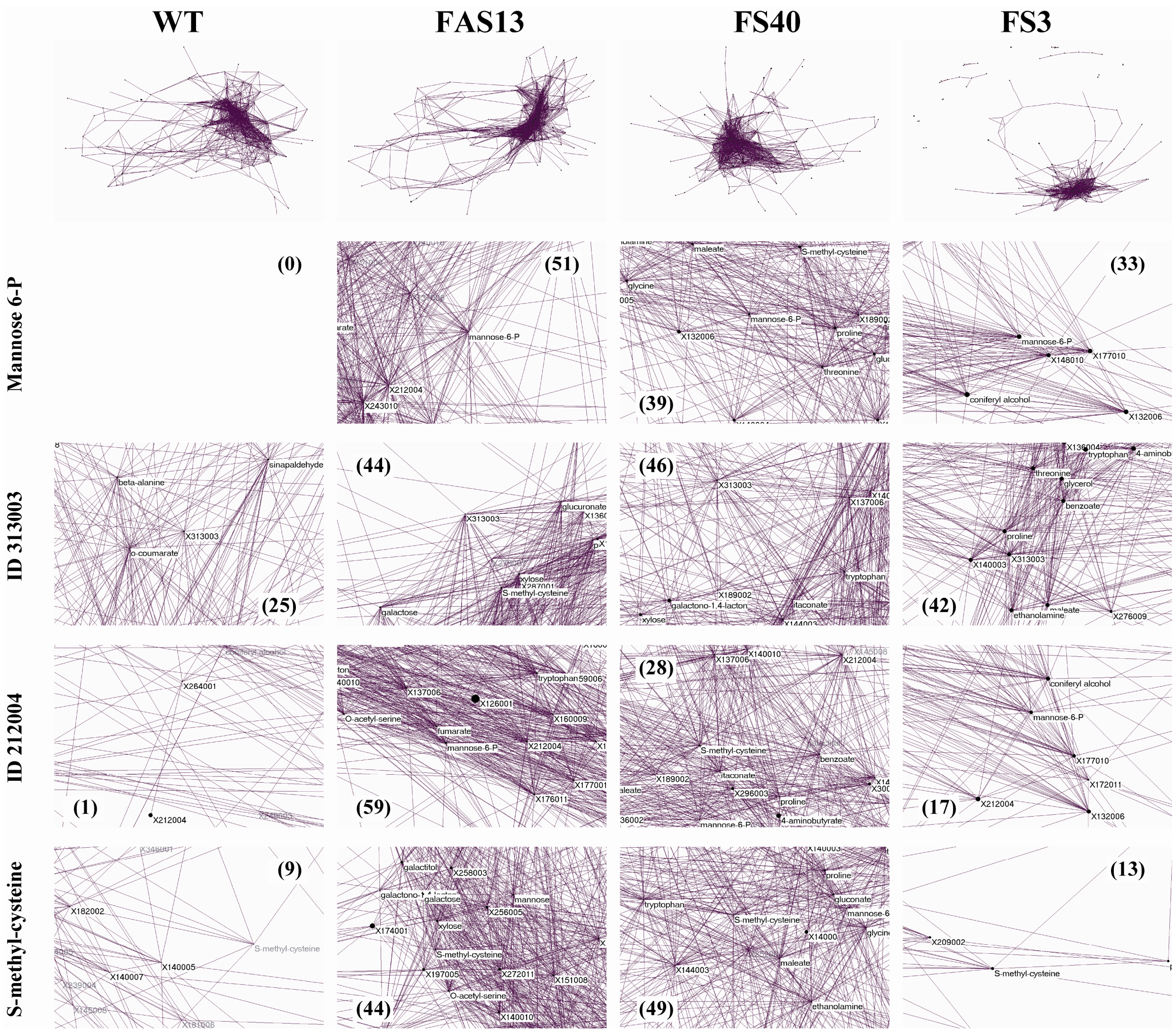
WT
FAS13
FS40
FS3
Mannose 6-P
ID 313003
ID 212004
S-methyl-cysteine
(0)
(51)
(39)
(33)
(25)
(44)
(46)
(42)
(1)
(59)
(28)
(17)
(9)
(44)
(49)
(13)
mannose-6-P
X212004
X243010
maleate
S-methyl-cysteine
glycine
X132006
proline
threonine
X148010
X177010
coniferyl alcohol
beta-alanine
sinapaldehyde
X313003
o-coumarate
glucuronate
xylose
galactose
galactono-1,4-lacton
X189002
itaconate
tryptophan
glycerol
benzoate
X140003
ethanolamine
X276009
X264001
X137006
X126001
O-acetyl-serine
fumarate
X160009
X176011
X140010
X296003
4-aminobutyrate
X172011
X182002
X140005
X140007
X258003
mannose
X256005
X174001
X197005
X272011
X151008
gluconate
X144003
X209002

Supplemental Figure 6. Metabolite correlation networks in WT and *CCR*-down-regulated poplar lines.

Networks were based on the strongly correlated GC-MS peaks (r>0.80) and generated with the Fruchtermann-Reingold three-dimensional algorithm. Metabolite correlation networks have a scale-free topology (Jeong et al., 2000) in which a small number of vertices ('hubs') are highly connected, whereas most have fewer connections. Removing a vertex will not alter the network topology as long as it is not a hub. As a consequence, scale-free networks are robust networks. Details of the networks, showing metabolites of which the number of strong correlations (in brackets) was clearly different in the transgenic lines as compared to WT, were enlarged.

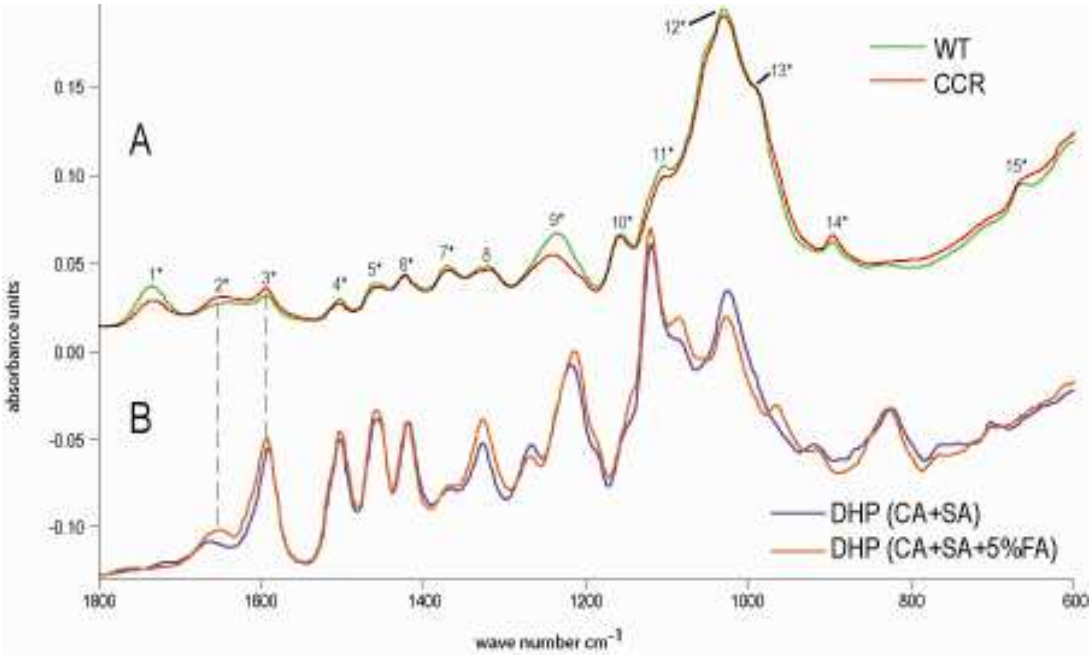

Supplemental Figure 7. FTIR spectrum overlay.

(A) Overlay of normalized FTIR spectra of xylem of WT (green, average of 12 measurements) and of intensely orange-brown colored xylem of *CCR*-down-regulated transformants (red, average of three measurements in FAS13 and two measurements in FS3). Absorption bands that were analyzed were numbered; an asterisk indicates absorption bands with significantly differential areas in the transformants when compared to WT.

(B) Overlay of normalized FTIR spectra of synthetic lignin made with ~50:50 coniferyl:sinapyl alcohols (purple, CA+SA) and of synthetic lignin made with 50:50 coniferyl:sinapyl alcohols and 5% ferulic acid (orange-brown, CA+SA+5%FA).

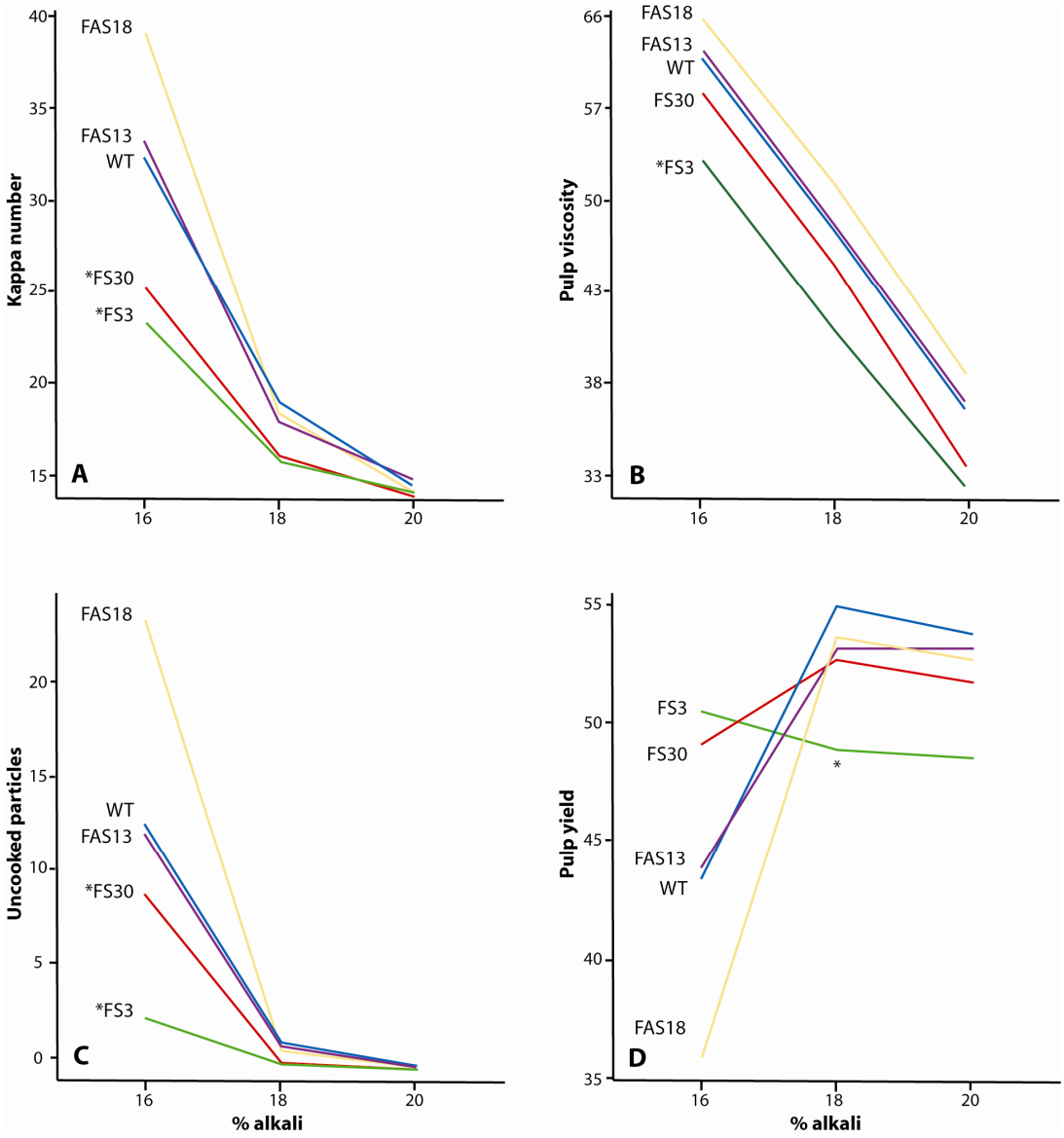

Supplemental Figure 8. Chemical pulping characteristics of field-grown *CCR*-down-regulated transgenic poplars

Pulping of 4-year-old trunks of WT and *CCR*-down-regulated poplars was assessed at three different alkali charges. **(A)** Kappa number. **(B)** Pulp viscosity (cP). **(C)** Uncooked particles. **(D)** Screened pulp yield. Data are means of five biological replicates. Lines for which the given pulping characteristic was significantly differential to the WT or single values that were significantly differential compared to WT are marked by an asterisk.

SUPPLEMENTAL TABLES

Supplemental Table 1. Transcript abundance percentage of the endogenous *CCR* gene in suppressed-CCR samples compared to WT. sem, standard error of the mean

Samples	Mean	sem
WT	100	4,45
FAS13 colorless	35,26	7,52
FAS13 colored	14,57	7,96
FS3 colored	3,45	2,09

Supplemental Table 2. Lignin profile in young developing xylem of WT and *CCR*-down-regulated poplars

						Lignin units														
Line	*Growth condition*	*Color*		*n*	*%Klason*	*PB*	*G*	*S*	*S+G*	*S/G*	*G-CHR-CHR2*	*Ferulate*	***X1γ***	*β–O–4*	*5–5*	*4–O–5*	*β–1*	*β–5*	*β–β*	*Total*
A. Klason lignin and thioacidolysis																				
WT	2yf	-		3	19.34 (0.23)				2636 (49)	2.12 (0.04)	2.24 (0.01)	Tr								
FS3	2yf	+		6	**10.18 (0.23)**				**2162 (53)**	2.38 (0.03)	**20.67 (1.24)**	**6.43 (0.22)**								
FS30	2yf	+		6	19.09 (0.27)															
FAS13	2yf	+		3	**14.81 (0.43)**															
FAS18	2yf	+		3	**17.94 (0.23)**															
FS3	1yg	-		1	19.35				***2041***	***2.23***	***3.4***									
		+		1	13.56				***1663***	***2.36***	***9.2***									
FS40	1yg	-		1	19.09				***2154***	***2.34***	1.87									
		+		1	15.02				***1808***	***2.64***	***7.1***									
B. Thioacidolysis from extractive-free xylem (EFX) and from the corresponding milled-wood extracted lignins (EL)																				
WT	1yg	-	EFX	3					2530 (30)	1.84 (0.08)	1.1 (0.3)	0.26 (0.01)			16.0 (0.5)	20.8 (0.6)	79.9 (2.7)	50.6 (1.1)	50.9 (1.1)	218 (6)
	1yg	-	EL	1					*1760 (53)*	*1.99 (0.02)*	*1.4 (0.1)*	*0.41 (0.04)*			*18 (1)*	*10.8 (0.1)*	*41.9 (0.6)*	*30.3 (0.3)*	*35 (0.5)*	*136 (3)*
FS3	1yg	+	EFX	3					2290 (150)	1.99 (0.06)	**12.9 (1.3)**	**2.0 (0.2)**			15.6 (3.1)	20.1 (1.6)	70.2 (4.9)	50.8 (2.0)	**35.8 (3.6)**	193 (15)
	1yg	+	EL	1					*1410 (34)*	*2.05 (0.02)*	*6.2 (0.4)*	*1.06 (0.3)*			*15.9 (0.2)*	*10.3 (1)*	*39.5 (2)*	*27.5 (1.5)*	*18 (2)*	*111 (6)*
C. NMR data obtained from EL and whole cell wall (wCW)																				
WT		-	EL	3		2.3 (0.3)	34.3 (1.2)	65.7 (1.2)		1.92 (0.10)			3.5 (0.6)	79.8 (0.8)			3.2 (1.0)	3.6 (0.4)	10.0 (0.8)	
		-	wCW	3		1.1 (0.6)	37.1 (0.4)	62.9 (0.4)		1.69 (0.03)			5.5 (1.3)	81.1 (0.6)			0.8 (0.6)	2.8 (0.6)	9.7 (0.2)	
FS40		-/+	EL	2		**3.1 (0.7)**	**38.1 (1.3)**	**61.9 (1.3)**		**1.63 (0.09)**			3.0 (0.6)	**83.1 (1.3)**			3.7 (0.1)	3.5 (0.4)	**6.8 (0.5)**	
		-/+	wCW	2		**2.9 (0.1)**	**42.4 (0.4)**	**57.6 (0.4)**		**1.36 (0.02)**			5.9 (0.1)	**84.4 (0.6)**			0.6 (0.6)	2.0 (0.6)	**7.0 (0.5)**	
FAS13		-/+	EL	2		3.1 (0.2)	**42.7 (0.8)**	**57.3 (0.8)**		**1.34 (0.04)**			4.2 (0.1)	**84.4 (0.7)**			2.0 (0.1)	4.0 (0.4)	**5.4 (0.3)**	
		-/+	wCW	2		1.9 (0.4)	**45.7 (1.3)**	**54.3 (1.4)**		**1.19 (0.06)**			7.7 (0.3)	**82.6 (0.3)**			2.4 (0.4)	2.0 (0.4)	**5.3 (0.7)**	

Samples of two-years-old field-grown poplars (2yf) were prepared from orange-brown young developing xylem, scraped from branches of the transgenic lines and from equivalent material harvested from WT poplars. Samples of one-year-old greenhouse-grown poplars (1yg) were prepared from young developing xylem, scraped separately from whitish and orange-brown areas in the stem for (A). The mean obtained from *n* biological replicates is given. The standard error of the mean (sem) is mentioned between brackets. Klason lignin content (%Kl) is expressed as weight percentage of extractive-free sample (EFX). Thioacidolysis yield of lignin units of milled-wood extracted lignins (EL), is expressed in µmoles per gram of Klason lignin. Each biological replicate was subjected to duplicate Klason analysis (sem from analytical replicates < 0.3%). Thioacidolysis was only run in duplicate when no biological replicate was available (sem from analytical replicates < 5%). All NMR data but the S/G ratio are expressed as percentages. NMR peaks obtained for *p*-hydroxybenzoate (PB), guaiacyl (G) and syringyl (S) were divided by the NMR peaks for G and S, and NMR data given for cinnamyl alcohol endgroups (**X1**γ), β–O–4 (β-aryl ether **A**), β–1 (spirodienone **S**), β–5 (phenylcoumaran **B**) and β–β (resinol **C**) are expressed relative to the sum of these five units. Klason lignin data, lignin results from EFX and EL, and NMR data were analyzed by t-tests and ANOVA (see Methods). Values that are significantly ($P<0.05$) different from WT and mean values and their sem that are solely based on technical replications are indicated in bold and italics, respectively. Bold italics is applied for thioacidolysis results on one-year-old greenhouse-grown poplars whenever the data are in agreement with results obtained on two-year-old field-grown poplars. β–β expresses syringaresinol and the total resinol amount in the case of thioacidolysis and NMR data, respectively. Tr, trace level; wCW, whole cell wall. -, -/+ and + indicate no, weak and strong coloration.

Supplemental Table 3. Weighted t-tests and ANOVA models of lignin analysis data of transgenic and WT poplars.

Trait	Model	P_{model}	P_{line}	$P_{factor2}$	$P_{interaction}$	$P_{coefficient}$
Klason lignin						
	Two-way	< 0.001	< 0.001	n.s.	n.s.	FS3 (< 0.001), FAS13 (< 0.001), FAS18 (< 0.001)
Thioacidolysis						
G+S	t-test	< 0.05				FS3
S/G	t-test	n.s.				
G-CHR-CHR2	t-test	< 0.001				FS3
NMR						
PB	Two-way	< 0.05	< 0.05	< 0.05	n.s.	FS40 (< 0.05)
G	Two-way	< 0.001	< 0.001	< 0.001	n.s.	FAS13 (< 0.001), FS40 (< 0.001)
S	Two-way	< 0.001	< 0.001	< 0.001	n.s.	FAS13 (< 0.001), FS40 (< 0.001)
S/G	Two-way	< 0.001	< 0.001	< 0.01	n.s.	FAS13 (< 0.001), FS40 (< 0.001)
β–O–4	Two-way	< 0.05	< 0.01	n.s.	n.s.	FAS13 (< 0.01), FS40 (< 0.01)
β–5	Two-way	< 0.05	n.s.	< 0.01	n.s.	
β–β	Two-way	< 0.001	< 0.001	n.s.	n.s.	FAS13 (< 0.001), FS40 (< 0.001)
Ferulate/sinapate	Two-way	n.s.				
X1γ	Two-way	< 0.001	n.s.	< 0.001	n.s.	
Cellulose/xylan	One-way	n.s.				
Polysaccharides/lignin	One-way	n.s.				
Mannan/(glucan+xylan)	One-way	n.s.				

Klason lignin ($n_{WT} = n_{FAS13} = n_{FAS18} = 3$; $n_{FS3} = n_{FS30} = 6$) and NMR data ($n_{WT} = 3$; $n_{FS40} = n_{FAS13} = 2$) were subjected to ANOVA, whereas a t-test was applied to analyze thioacidolysis data ($n_{WT} = 3$; $n_{FS3} = 6$). Two experiments were performed to determine the Klason lignin content. For all but the polysaccharides, NMR data were recorded for the enzyme lignins (EL) and whole cell walls (wCW). Factor2 is experiment and method in the case of Klason lignin content and NMR data, respectively. The WT and the EL-based method were the reference category for the line and method effect, respectively. Red and green indicate significantly increased and decreased abundances. All threshold significances of the two-way ANOVA models but the interaction effect (α=0.01) were 0.05. The significance of the coefficient factor was derived from LSD and Wald tests for Klason lignin and NMR data, respectively. Klason lignin content (%Kl) is expressed as weight percentage of extractive-free sample. Thioacidolysis yield of monomers is expressed in µmoles per gram of Klason lignin. All NMR data, but the S/G ratio, were expressed as percentages. Percentages were angular transformed before analysis. All traits were sufficiently homoscedastic. NMR peaks obtained for *p*-hydroxybenzoate (PB), guaiacyl (G) and syringyl (S) were divided by the NMR peaks for G and S, and NMR data given for ferulate/sinapate, cinnamyl alcohol endgroups (X1γ), β–O–4, β–5 and β–β are expressed relative to the sum of these five units.

Supplemental Table 4. Concentration of phenylpropanoids identified in *CCR*-down-regulated and control poplars (mean pmole/mg dry weight ± sem)

Compound	Control			*CCR*-down-regulated			Fold change
	WT	35S 17B	35S 21B	FS3	FS40	FAS13	
	n=5	n=6	n=8	n=4	n=4	n=6	
GVA	246 ± 30	227 ± 20	214 ± 20	**5820 ± 1000**	**4250 ± 1200**	**6130 ± 2500**	24
GSA	n.d.	n.d.	n.d.	**3700 ± 700**	**1960 ± 600**	**2320 ± 1000**	1000
G(*t*8–O–4)**G***	69.5 ± 31	38.8 ± 29	94.3 ± 40	194 ± 30	82.7 ± 40	217 ± 50	
G(8–5)**G**	105 ± 40	95.5 ± 28	98.1 ± 24	**7.73 ± 3.1**	**38.7 ± 23**	**27.0 ± 13**	0.25
G(8–8)**G**	53.3 ± 8	46.5 ± 3	42.2 ± 5	17.3 ± 9.0	39.0 ± 4	31.0 ± 13	
S(8–8)**S**	coel.	coel.	coel.	n.d.	coel.	coel.	
S(8–5)**G**	41.3 ± 6	31.2 ± 9	39.3 ± 5	n.d.	**15.8 ± 6**	**16.7 ± 6**	0.31
G(8–5)**V'**	n.d.	n.d.	n.d.	n.d.	n.d.	n.d.	
G(8–5)**G'**	13.5 ± 7	2.52 ± 0.4	4.64 ± 1.2	2.95 ± 0.7	4.86 ± 2.5	2.70 ± 0.4	
G(*t*8–O–4)**G**(t8–O–4)**G**	20.4 ± 4	15.6 ± 7	23.3 ± 5	n.d.	6.65 ± 2.9	6.60 ± 1.9	
S(*t*8–O–4)**S**(8–5)**G**	n.d.	n.d.	n.d.	n.d.	n.d.	n.d.	
G(t8–O–4)**S**(8–5)**G**	151 ± 30	153 ± 30	152 ± 20	**6.12 ± 3.2**	**57.4 ± 21**	**66.6 ± 22**	0.29
G(*e*8–O–4)**S**(8–5)**G**	35.7 ± 4	37.7 ± 7	34.9 ± 6	n.d.	**11.0 ± 6**	**16.4 ± 7**	0.16
S(*t*8–O–4)**S**(8–5)**G'**	coel.	coel.	coel.	n.d.	coel.	coel.	
SP(8–8)**S**	20.3 ± 6	27.2 ± 5	24.4 ± 6	n.d.	**7.30 ± 3.5**	7.74 ± 4.0	0.25
G(*t*8–O–4)**S**(8–5)**G'**	107 ± 10	125 ± 20	96.0 ± 13	**12.4 ± 1**	**39.6 ± 13**	**44.2 ± 19**	0.29
G(*e*8–O–4)**S**(8–5)**G'**	85.8 ± 7	92.9 ± 25	82.1 ± 13	**6.20 ± 2.6**	**31.4 ± 10**	**35.7 ± 19**	0.28
G(8–O–4)**S**(8–8)**S**(8–O–4)**G**	66.4 ± 6	65.0 ± 11	67.5 ± 6	**25.4 ± 5**	**34.5 ± 6**	**58.6 ± 13**	0.60

Mean concentrations of phenylpropanoids, expressed as pmole/mg dry weight, are shown for the control poplar lines (WT, transgenic lines 35S 17B and 35S 21B) and *CCR*-down-regulated poplar lines (FS3, FS40, and FAS 13). The fold change of the product abundance in *CCR*-down-regulated poplars relative to the control lines is indicated. When the compound was not detected by HPLC-UV/Vis, the relative increase was calculated with a detection limit of 2.6 pmole/mg dry weight. Significantly different concentrations between control and *CCR*-down-regulated poplars are shown in bold. In addition to the eight differentially

accumulating oligolignols in *CCR*-down-regulated poplars, oligolignols that have been previously annotated in HPLC chromatograms of xylem extracts are shown as well. For nomenclature of the peaks, see Morreel et al. (2004a). Data are means ± sem from biological replicates. n, number of biological replicates; coel., concentration not determined due to co-elution of two or more compounds; n.d., not detected; *, difficult to quantify due to co-elution.

Supplemental Table 5. Identity, expression pattern and functional classification of the genes identified for their differential expression in the xylem of WT and the *CCR*-down-regulated transformants FS3 and FS40 by hybridization with the POP2 poplar microarray

Clone ID	*Arabidopsis* ortholog (AGI)	Description	Transcript level over WT	
			FS3	FS40
PU03786	At3g61220	Short-chain dehydrogenase/reductase (SDR) family protein similar to carbonyl reductase GI:1049108 from [*Mus musculus*]	**2.02919**	**1.531**
PU01618	At5g37600	Glutamine synthetase, putative	**1.37563**	**1.37042**
PU20678	At3g10870		**1.8169**	**1.5938**
PU08212	At5g63310	Nucleotide diphosphate kinase II, chloroplast (NDPK2) identical to SP|O64903 Nucleoside diphosphate kinase II, chloroplast precursor (NDK II) (NDP kinase II) (NDPK II) (NDPK Ia) [*Arabidopsis thaliana*]	**1.54912**	**1.63162**
PU06825	At1g19300	Glycosyl transferase family 8 protein contains Pfam profile: PF01501 Glycosyl transferase family 8	*0.67104*	*0.71644*
PU10485	At1g19300	Glycosyl transferase family 8 protein contains Pfam profile: PF01501 Glycosyl transferase family 8	*0.63905*	*0.72246*
PU29383	At1g14520	Oxygenase-related similar to myo-inositol oxygenase [*Sus scrofa*] gi|17432544|gb|AAL39076	*0.41824*	*0.61727*
PU07781	At1g30620	UDP-D-xylose 4-epimerase, putative (MUR4) similar to SP|P55180 UDP-glucose 4-epimerase (EC 5.1.3.2) from *Bacillus subtilis*, GI:3021357 UDP-galactose 4-epimerase from *Cyamopsis tetragonoloba*; contains	*0.74344*	*0.82482*
PU26373	At5g01930	(1-4)-β-Mannan endohydrolase, putative similar to (1-4)-β-mannan endohydrolase [*Coffea arabica*] GI:10178872; contains Pfam profile PF00150: cellulase (glycosyl hydrolase family 5)	**1.8823**	**1.95956**
PU02921	At1g75130	Cytochrome P450 family protein similar to Cytochrome P450 72A1 (SP:Q05047) [*Catharanthus roseus*]	**1.56901**	**1.34664**
PU25384	At5g63450	Cytochrome P450, putative	**1.87219**	**1.41102**
PU22278;	At2g37040	Phenylalanine ammonia-lyase 1 (PAL1) nearly identical to	**2.59**	**2.30**

PU30088		SP|P35510		
PU20140	At2g37040	Phenylalanine ammonia-lyase 1 (PAL1) nearly identical to SP|P35510	**2.07963**	**1.78094**
PU00591; PU01488; PU01628; PU03517	At1g15950	Cinnamoyl-CoA reductase, putative nearly identical to CCR1 (GI:12034897), similar to cinnamoyl CoA reductase GI:2058310 from [*Eucalyptus gunnii*]	*0.44*	*0.56*
PU22661	At5g38900	DSBA oxidoreductase family protein contains Pfam profile: PF01323 DSBA-like thioredoxin domain	**1.46005**	**1.46547**
PU06943	At5g40760	Glucose-6-phosphate 1-dehydrogenase / G6PD (ACG12) idential to glucose-6-phosphate 1-dehydrogenase (acg12) [*Arabidopsis thaliana*] GI:5732197	**1.54679**	**1.43303**
PU10952	At4g15510	Photosystem II reaction center PsbP family protein contains PsbP domain PF01789; identical to SP:O23403 [*Arabidopsis thaliana*]	**2.81855**	**1.63368**
PU02476	At5g55190	Ras-related GTP-binding protein (RAN3) identical to atran3 [*Arabidopsis thaliana*] GI:2058280	**1.23856**	**1.16068**
PU30087	At2g02470	PHD finger family protein contains Pfam domain, PF00628: PHD-finger	**1.14305**	**1.30266**
PU09933	At3g21890	Zinc finger (B-box type) family protein contains Pfam profile: PF01760 CONSTANS family zinc finger	*0.45093*	*0.60626*
PU31165	At5g57150	Basic helix-loop-helix (bHLH) family protein contains Pfam profile: PF00010 helix-loop-helix DNA-binding domain	*0.42582*	*0.48384*
PU25316	At2g16600	Peptidyl-prolyl cis-trans isomerase, cytosolic/cyclophilin/rotamase (ROC3) identical to cytosolic cyclophilin [*Arabidopsis thaliana*] GI:1305455	**1.65763**	**1.40284**
PU26727	At3g18710	U-box domain-containing protein similar to immediate-early fungal elicitor protein CMPG1 [*Petroselinum crispum*] GI:14582200; contains Pfam profile PF04564: U-box domain	**1.9251**	**1.34808**
PU28456	At3g45010	Serine carboxypeptidase III, putative similar to serine	**1.96752**	**1.75588**

		carboxypeptidase III from *Oryza sativa* SP|P37891, *Matricaria chamomilla* GI:6960455, *Hordeum vulgare* SP|P21529, *Triticum aestivum* SP|P11515; cont		
PU04416	At5g16760	Inositol 1,3,4-trisphosphate 5/6-kinase identical to inositol 1,3,4-trisphosphate 5/6-kinase GI:3396079 from [*Arabidopsis thaliana*]	**1.52232**	**1.25598**
PU12664	At2g40120	Protein kinase family protein contains protein kinase domain, Pfam:PF00069	*0.70792*	*0.83343*
PU11549	At3g43740	Leucine-rich repeat family protein contains leucine rich-repeat (LRR) domains Pfam:PF00560, INTERPRO:IPR001611; contains similarity to somatic embryogenesis receptor-like kinase 2 [*Arabidopsis thaliana*] gi|14573457|gb|AAK68073 (At1g34210)	**1.73404**	**1.31664**
PU06451	At5g16590	Leucine-rich repeat transmembrane protein kinase (LRR III), putative	*0.71292*	*0.69877*
PU09992	At3g09390	Metallothionein protein, putative (MT2A) identical to Swiss-Prot:P25860 metallothionein-like protein 2A (MT-2A) (MT-K) (MT-1G) [*Arabidopsis thaliana*]	**2.79698**	**1.60838**
PU10380; PU20342; PU29478; PU29522; PU29583	At3g09390	Metallothionein protein, putative (MT2A) identical to Swiss-Prot:P25860 metallothionein-like protein 2A (MT-2A) (MT-K) (MT-1G) [*Arabidopsis thaliana*]	**2.94**	**1.75**
PU11789	At3g09390	Metallothionein protein, putative (MT2A) identical to Swiss-Prot:P25860 metallothionein-like protein 2A (MT-2A) (MT-K) (MT-1G) [*Arabidopsis thaliana*]	**3.12688**	**1.66709**
PU25376; PU27888; PU27899; PU28089	At3g09390	Metallothionein protein, putative (MT2A) identical to Swiss-Prot:P25860 metallothionein-like protein 2A (MT-2A) (MT-K) (MT-1G) [*Arabidopsis thaliana*]	**2.83**	**1.85**
PU12564	At1g26320	NADP-dependent oxidoreductase, putative similar to probable	**2.95306**	**1.59815**

		NADP-dependent oxidoreductase (zeta-crystallin homolog) P1 [SP|Q39172][gi:886428] and P2 [SP|Q39173][gi:886430], *Arabidopsis thaliana*		
PU26711; PU29472	At2g47730	Glutathione-*S*-transferase 6 (GST6) identical to GB:X95295. Based on identical cDNA hits, the translation is now 40 AAs longer at the N-terminal, and start of exon2 is also corrected. GST class phi	**2.37**	**1.56**
PU04942	At3g09270	Glutathione-*S*-transferase, putative similar to glutathione transferase GB:CAA71784 [*Glycine max*] ATGSTU8 Encodes glutathione transferase belonging to the tau class of GSTs. Naming convention according to Wagner et al. (2002)	**2.73111**	**2.11629**
PU20278	At5g11740	Arabinogalactan-protein AGP15	*0.61131*	*0.71845*
PU05093	At4g39080	Vacuolar proton ATPase, putative similar to Swiss-Prot:Q93050 vacuolar proton translocating ATPase 116 kDa subunit A isoform 1 (Clathrin-coated vesicle/synaptic vesicle proton pump 116 kDa subunit, Va	**1.60226**	**1.28383**
PU21070	At3g22600	Protease inhibitor/seed storage/lipid transfer protein (LTP) family protein contains Pfam protease inhibitor/seed storage/LTP family domain PF00234	*0.52298*	*0.65103*
PU07796	At2g29130	Laccase, putative / diphenol oxidase, putative similar to laccase [*Liriodendron tulipifera*][GI:1621467]	*0.65947*	
PU09268	At4g30210	NADPH-cytochrome p450 reductase, putative / NADPH-ferrihemoprotein reductase, putative similar to NADPH-cytochrome P450 oxydoreductase from [*Populus balsamifera* subsp. *trichocarpa x P. deltoides*]	**1.45716**	**1.40881**
PU08734	At4g35110	Expressed protein	**1.19043**	*0.85527*
PU10623	At5g65960	Expressed protein	*0.58385*	
PU27262	At4g20260	DREPP plasma membrane polypeptide family protein contains Pfam profile: PF05558 DREPP plasma membrane polypeptide	*0.55505*	

PU13267	At3g19000		**1.90668**	**1.73473**
PU01498	At1g06920	Ovate family protein 58% similar to ovate protein (GI:23429649) [*Lycopersicon esculentum*]; contains TIGRFAM TIGR01568 : uncharacterized plant-specific domain TIGR01568	*0.58667*	*0.619*
PU20721	At1g09980	Expressed protein contains Pfam profile PF05057: Protein of unknown function (DUF676); non-consensus GC donor splice site at exon boundary 144764	*0.78711*	*0.80087*
PU27583	At1g74450	Expressed protein	*0.47776*	*0.51537*
PU12872	At2g01100	Expressed protein	*0.51569*	*0.55537*
PU10465	At3g29780	Expressed protein	**2.25639**	**1.44163**
PU05035	At3g48380	Expressed protein	**2.21751**	**1.50617**
PU30713	At4g32020	Expressed protein NuLL	*0.58138*	*0.60647*
PU04599	At1g60985	Hypothetical protein SCRL6 [Precursor]	**2.71036**	**1.72986**

The PU numbers refer to the DNA preparations spotted on the microarray. The description of the genes was retrieved from PopulusDB (www.populus.db.umu.se). From the best Arabidopsis match, a functional classification was retrieved from the Munich Information Centre for Protein Sequences (MIPS) database (mips.gsf.de) and this functional classification was subsequently manually curated. Transcript levels are given as a fold-change of WT levels. Font in italics and underlined indicates reduced transcript levels, bold font indicates increased transcript levels. AGI, Arabidopsis Genome Initiative.

Supplemental Table 6. Number of vertices and edges composing the correlation networks

	WT	*FAS13*	*FS40*	*FS3*
# vertices	190	197	188	143
# edges	1582	1909	1482	830
# edges/vertex	8.3	9.7	7.9	5.8

Supplementary Table 7. Carbohydrate analyses raw data

Sample		Quantity of each monomer from isolated hemicellulose (mg)						Total Hemicellulose
Line	Replicate	Ara	Rha	Gal	Glu	Xyl	Man	(mg)
FS3	1	0.11	0.28	0.35	1.87	18.40	1.11	22.12
	2	0.10	0.27	0.34	1.76	21.23	1.10	24.81
	3	0.13	0.28	0.35	1.42	19.14	1.04	22.36
	4	0.15	0.30	0.40	1.94	21.00	1.17	24.97
	5	0.10	0.30	0.39	1.45	18.54	0.89	21.68
FS40	1	0.13	0.32	0.44	1.76	19.53	0.99	23.17
	2	0.11	0.33	0.38	2.06	20.03	1.21	24.12
	3	0.13	0.29	0.44	2.36	20.23	1.16	24.62
	4	0.11	0.33	0.40	1.80	21.69	1.13	25.45
	5	0.15	0.29	0.41	1.59	19.63	1.05	23.12
WT	1	0.14	0.42	0.52	3.16	24.85	1.71	30.80
	2	0.11	0.42	0.50	2.73	22.16	1.49	27.40
	3	0.17	0.41	0.53	2.87	26.31	1.63	31.91
	4	0.15	0.47	0.53	3.17	25.48	1.64	31.43
	5	0.15	0.47	0.50	3.09	25.84	1.70	31.74
	6	0.12	0.43	0.47	2.58	25.83	1.60	31.03

Quantities are derived from the extraction of 100 mg holocellulose (see Methods). Ara, arabinose; Gal, galactose; Glu, glucose; Man, mannose; Rha, rhamnose; Xyl, xylose.

Supplemental Table 8. ANOVA models for FTIR data of transgenic and wild type poplars

	Wavelength range (cm^{-1})	P_{model}	$P_{individual|line}$	P_{line}	P_{color}	Cell wall property
1	1778-1691	< 0.001	< 0.001 (FS3)	n.s.	< 0.001	Carbohydrate, ester
2	1691-1612	< 0.001	< 0.01 (FS3)	n.s.	< 0.001	Aromatic conjugated carbonyl
3	1612-1554	< 0.001	< 0.001 (FS3)	n.s.	< 0.001	Lignin
4	1527-1486	< 0.001	< 0.001 (FS3/FAS13)	< 0.001 (FS3)	< 0.001	Lignin
5	1486-1442	< 0.001	< 0.001 (FAS13)	< 0.001	< 0.001	Lignin and Carbohydrate
6	1442-1397	< 0.01	n.s.	< 0.001 (FS3)	n.s.	Lignin and Carbohydrate
7	1397-1349	< 0.001	< 0.01 (WT/FS40)	< 0.05 (FS3)	< 0.001	Carbohydrate
8	1349-1293	n.s.	n.s.	n.s.	n.s.	Lignin and Carbohydrate
9	1293-1188	< 0.001	< 0.001 (FS3)	< 0.01 (FS40)	< 0.001	Lignin and Carbohydrate
10	1188-1145	< 0.001	< 0.01 (WT)	< 0.01 (FS3)	< 0.001	Carbohydrate
11	1145-1096	< 0.001	< 0.001 (FS3)	< 0.001 (FS40)	< 0.001	Lignin and Carbohydrate
12	1096-999	< 0.001	< 0.001 (WT/FS3/FS40/FAS13)	< 0.01	< 0.001	Carbohydrate
13	999-917	< 0.001	< 0.001 (WT/FS3/FS40/FAS13)	< 0.01	< 0.001	Carbohydrate
14	917-881	< 0.001	< 0.001 (WT/FS3/FS40/FAS13)	< 0.01 (FS3)	< 0.001	Carbohydrate
15	683-649	< 0.001	n.s.	< 0.001 (FS40)	< 0.001	No assignment

Data were obtained for four individuals of the FS3 (all slightly red), FS40 (three slightly red and one whitish individuals), FAS13 (three whitish and one intensely red) transgenic and the control poplars. Three different stem sections were measured for each individual. Poplar lines responsible for a significant nested effect ($P_{individual|line}$, α=0.01) are mentioned between brackets. A significant positive or negative association between the absorption band and the reddish color intensity (P_{color}, α=0.05) is shown in red or green, respectively. Transgenic lines that show a significant line effect (P_{line}, α=0.05) are mentioned between brackets. Taking the color effect into account, a positive or negative line effect relative to wild type is indicated in red or green, respectively. n.s., not significant. Absorption bands 1, 7, 10 and 12 have been previously associated with cell wall carbohydrates (Michell, 1989; McCann et al., 1992; Kacuráková et al., 2002; Mouille et al., 2003; 2006; Pandey and Pitman, 2003) and, more specifically, with ester groups of xylans and pectins in the case of absorption band 1 (Faix, 1991; Séné et al., 1994; Mouille et al., 2003; Pandey and Pitman, 2003; Labbé et al., 2005). Absorption band 2 has been associated with aromatic compounds and bands 3 and 4 with lignin (Faix, 1991; Stewart et al., 1997; Zhong et al., 2000; Pandey and Pitman, 2003; Xu et al., 2005; Sibout et al., 2005).

SUPPLEMENTAL METHODS

Statistical analysis of Klason lignin data

Because Klason lignin in young xylem was measured twice, significant differences between the poplar lines (α_{model} = 0.05; α_{line} = 0.05) were determined by a two-way ANOVA. No significant batch × experiment interaction was observed ($\alpha_{interaction}$ = 0.01). Klason lignin results of all xylem tissues as well as thioacidolysis results were subjected to a one-way ANOVA or an independent samples t-test to reveal significant differences between poplar lines (α_{model} = 0.05). Whenever a significant difference was found with ANOVA, a least significant difference (LSD) post-hoc test was applied (α_{LSD} = 0.05). All analyses were done with SPSS 12.0.

Statistical analysis of cellulose, hemicellulose, acid-soluble and acid-insoluble Klason lignin, and the hemicellulose-derived sugar ratios

The analyses were performed with R version 2.4.0. Significant differences (α=0.05) between the poplar lines were determined with a nested ANOVA or, whenever there was a non-significant (α=0.01) nested effect, a one-way ANOVA model. Homoscedasticity was evaluated by modeling the absolute values of the residuals with the lm procedure. Proportions were subjected to an angular transformation before ANOVA.

Statistical analysis of the soluble phenolics

Concentrations of soluble phenolics in the different transgenic lines, as measured by peak height divided by dry weight, were compared with those in WT with a nested ANOVA or a one-way ANOVA model according to the conditions described in Morreel et al. (2004b) with the software program SPSS 12.0.

Statistical analysis of microarray data

The microarray data were transformed logarithmically (base 2) and normalized with the Lowess macro implemented in the SAS system applying a linear function for the local regression and an f-value (window width) of 0.50. MA plots were constructed according to Dudoit et al. (2002) (data not shown) and data were analyzed according to Wolfinger et al. (2001) with two interconnected ANOVA models. With the SAS proc mixed procedure the parameters in the ANOVA models were fitted. The REML (residual restricted maximum likelihood) method was used to estimate the covariance parameters. The normalization model applied was

$$y_{gijkl} = \mu + A_i + (AD)_{ij} + r_{gijkl}$$

where y_{gijk} is the base-2 logarithm of the Lowess-normalized intensity measurements from gene g (g=1,...,16133), array i (i=1,...,12), dye j (j=1,2), variety k (k=1,2,3), and biological replicate l (l=1,2). μ represents an overall mean value, A is the main effect for arrays, AD is the interaction effect between arrays and dyes, and r the residuals. We included no main effect for dyes, because the design was balanced in the dyes. The gene model at the gene level was

$$r_{gijkl} = G_g + (GA)_{gi} + (GD)_{gj} + (GV)_{gk} + (GR)_{gl} + \varepsilon_{gijkl}$$

where ε represents here the mean value per gene; GA, the gene-specific array effects reflecting the spot-to-spot variability inherent in spotted microarray data; GD, the gene-specific dye effects; V, the gene-specific variety effects; and R the gene-specific replicate effects. The biological replicate here is considered as a blocking factor. A_i, $(AD)_{ij}$ in the normalization model and $(GA)_{gi}$ in the gene model are random effects. The remaining effects are assumed to be fixed. For the gene model, type 3 tests of fixed effects (F-tests) containing hypothesis tests for the significance of each of the fixed effects along with p-values for these tests were calculated, as well as differences of the least-square means for the variety effects along with associated t-tests and p-values. The p-values of the type 3 tests of the variety effect were adjusted using the method of Benjamini and Hochberg (1995) to control the false discovery rate (FDR) with the SAS multitest procedure. A gene was considered to be differentially expressed when the fdr-adjusted p-value was < 0.001 and when the p-values for differences of the least square means between WT and FS3 or between WT and FS40 were significant at the 0.001 level.

Statistical analysis of GC-MS data

GC-MS data were subjected to a principal component analysis (PCA) with SPSS 12.0. Scatter plots were generated with S-Plus 6.1 (Insightful, Berlin, Germany). Compounds predominantly contributing to the principal components (PCs) were determined if the absolute value of their loading factor were larger than one standard deviation from the mean loading factor in the particular PC. No distinction between the WT and the transgenic poplars was obtained by each of the six highest-ranking PCs. Plotting of PC7 and PC8 two-dimensionally afforded a partial separation of WT and transgenic poplars, yet no distinction was observed when each of these PCs was considered independently. Therefore, only compounds that contributed predominantly in both PCs were considered responsible for separating transgenic and WT lines. PC9 was able to roughly separate WT and transgenic poplars. Together, PC7, PC8, and PC9 explained cumulatively 9% of the variance present in the dataset. Additionally, integrated m/z traces in GC-MS chromatograms were analyzed by means of t-tests to reveal significant differences (α=0.001 in at least one of the transgenic lines) in abundance between WT and *CCR* down-regulated poplars with the Excel 2000 software.

Statistical analysis of chemical pulping data

Because different alkali concentrations were used during pulping, the values of the pulping parameters, i.e. Kappa number, uncooked particles, screened pulp yield, and pulp viscosity were analyzed by a two-way ANOVA. In the case of a significant interaction term (α=0.01), a one-way ANOVA was applied. When appropriate, ANOVA was followed by an LSD post-hoc test. For all, but the interaction term, significance thresholds were set at 0.05. Box-Cox transformations were performed to obtain homoscedasticity.

Statistical analysis of growth data

Three-way ANOVA analyses involving clone, block and year effect, and all interactions were

conducted on height, girth, girth increase, calculated volume and volume increase, with Box-Cox transformations whenever necessary. After removing non-significant interactions ($\alpha = 0.01$), height ($R_{adj}^2 = 0.87$), girth ($R_{adj}^2 = 0.90$), volume ($R_{adj}^2 = 0.93$) and volume increase ($R_{adj}^2 = 0.65$) were modeled according to **1**, whereas the full model **2** was retained for girth increase ($R_{adj}^2 = 0.50$).

$$y_{ijkl} = \mu + yr_i + cl_j + bl_k + (cl \times bl)_{jk} + \varepsilon_{ijkl} \quad \textbf{1}$$

$$y_{ijkl} = \mu + yr_i + cl_j + bl_k + (yr \times bl)_{ij} + (yr \times bl)_{jk} + (yr \times cl \times bl)_{ijk} + \varepsilon_{ijkl} \quad \textbf{2}$$

where y_{ijkl} is the value of the trait in individual l belonging to the i^{th} year, the j^{th} clone and the k^{th} block; μ is the overall mean trait value; yr_i, cl_j and bl_k are the deviations from the overall mean due to the effect of the i^{th} year, j^{th} clone and k^{th} block, respectively; $(yr \times cl)_{ij}$, $(yr \times bl)_{ik}$, and $(cl \times bl)_{jk}$ are deviations from the overall mean resulting from two-way interactions; $(yr \times cl \times bl)_{ijk}$ is the deviation from the overall mean due to three-way interaction; ε_{ijkl} is the residual deviation of the trait value in individual j of the i^{th} year, the j^{th} clone, and the k^{th} block. The main effects were evaluated with the three possible two-way ANOVA models ($\alpha = 0.05$), i.e. based on year and clone, year and block and clone and block, whereby the first explained most of the variation for all traits. This two-way model with year and clone as main effects showed an insignificant interaction ($\alpha = 0.01$) for all analyzed traits. After a significant clone effect ($\alpha_{clone} = 0.05$), differences between each transgenic line and WT poplars were detected by an LSD post hoc test ($\alpha_{post\ hoc} = 0.05$).

Statistical analysis of FTIR data

For the different transgenic and WT poplar lines, a nested ANOVA was attempted because three stem sections were measured for each individual replicate. A highly significant nested effect obscured the determination of any significant transgenic line effect. This confounding effect was partially removed by incorporating the color of the section (0=white, 1=slightly orange-brown, and 2=intensely orange-brown) as a covariate in the ANOVA model **3**.

$$y_{ijkl} = \mu\ col_i + line_j + rep_{k|j} + \varepsilon_{ijkl} \quad \textbf{3}$$

where y_{ijkl} is the value of the trait in stem section l with the i^{th} color intensity and belonging to the k^{th} individual replicate given the j^{th} transgenic line; μ is the overall mean trait value; col_i, $line_j$ and $rep_{k|j}$ are the deviations from the overall mean due to the effect of the i^{th} color intensity, j^{th} transgenic line

and k^{th} individual replicate given the j^{th} transgenic line, respectively; ε_{ijkl} is the residual deviation of the trait value in stem section l of the i^{th} color, the j^{th} transgenic line, and the k^{th} individual given the j^{th} transgenic line. For all, but the nested effect ($\alpha = 0.01$), all thresholds were set at 0.05. Residual plots revealed a constant error variance. Statistical analyses of all FTIR data were done with R version 2.2.1.

REFERENCES

Benjamini, Y., and Hochberg, Y. (1995). Controlling the false discovery rate: a practical and powerful approach to multiple testing. J. R. Stat. Soc. Ser. B-Stat. Methodol. **57,** 289-300.

Dudoit, S., Yang, Y.H., Callow, M.J., and Speed, T.P. (2002). Statistical method for identifying differentially expressed genes in replicated cDNA microarray experiments. Statist. Sin. **12,** 111-139.

Faix, O. (1991). Classification of lignins from different botanical origins by FT-IR spectroscopy. Holzforschung **45,** Suppl., 21-27.

Jeong, H., Tombor, B., Albert, R., Oltval, Z.N., and Barabási, A.-L. (2000). The large-scale organization of metabolic networks. Nature **407,** 651-654.

Kačuráková, M., Smith, A.C., Gidley, M.J., and Wilson, R.H. (2002). Molecular interactions in bacterial cellulose composites studied by 1D FT-IR and dynamic 2D FT-IR spectroscopy. Carbohydr. Res. **337,** 1145-1153.

Labbé, N., Rials, T.G., Kelley, S.S., Cheng, Z.-M., Kim, J.Y., and Li, Y. (2005). FT-IR imaging and pyrolysis-molecular beam mass spectrometry: new tools to investigate wood tissues. Wood Sci. Technol. **39**, 61-77

McCann, M.C., Hammouri, M., Wilson, R., Belton, P., and Roberts, K. (1992). Fourier transform infrared microspectroscopy is a new way to look at plant cell walls. Plant Physiol. **100,** 1940–1947.

Michell, A.J. (1989). Second derivative FTIR spectra of woods. In Cellulose and Wood Chemistry and Technology, Proceedings of 10th Cellulose Conference, Syracuse, NY, May 29-June 2, 1988, C. Schuerch, ed. (New York: Wiley), pp. 995-1008.

Morreel, K., Ralph, J., Kim, H., Lu, F., Goeminne, G., Ralph, S., Messens, E., and Boerjan, W. (2004a). Profiling of oligolignols reveals monolignol coupling conditions in lignifying poplar xylem. Plant Physiol. **136,** 3537-3549.

Morreel, K., Ralph, J., Lu, F., Goeminne, G., Busson, R., Herdewijn, P., Goeman, J.L., Van der Eycken, J., Boerjan, W., and Messens, E. (2004b). Phenolic profiling of caffeic acid *O*-methyltransferase-deficient poplar reveals novel benzodioxane oligolignols. Plant

Physiol. **136,** 4023-4036.

Mouille, G., Robin, S., Lecomte, M., Pagant, S., and Höfte, H. (2003). Classification and identification of *Arabidopsis* cell wall mutants using Fourier-Transform InfraRed (FT-IR) microspectroscopy. Plant J. **35,** 393–404.

Mouille, G., Witucka-Wall, H., Bruyant, M.-P., Loudet, O., Pelletier, S., Rihouey, C., Lerouxel, O., Lerouge, P., Höfte, H., and Pauly, M. (2006). Quantitative trait loci analysis of primary cell wall composition in Arabidopsis. Plant Physiol. **141,** 1035-1044.

Pandey, K.K., and Pitman, A.J. (2003). FTIR studies of the changes in wood chemistry following decay by brown-rot and white-rot fungi. Int. Biodeterior. Biodegrad. **52,** 151-160.

Séné, C., McCann, M.C., Wilson, R.H., and Grinter, R. (1994). Fourier-transform Raman and Fourier-transform infrared spectroscopy. An investigation of five higher plant cell walls and their components. Plant Physiol. **106,** 1623-1631.

Sibout, R., Eudes, A., Mouille, G., Pollet, B., Lapierre, C., Jouanin, L., and Séguin, A. (2005). *CINNAMYL ALCOHOL DEHYDROGENASE-C* and *-D* are the primary genes involved in lignin biosynthesis in the floral stem of Arabidopsis. Plant Cell **17,** 2059-2076.

Stewart, D., Yahiaoui, N., McDougall, G.J., Myton, K., Marque, C., Boudet, A.M., and Haigh, J. (1997). Fourier-transform infrared and Raman spectroscopic evidence for the incorporation of cinnamaldehydes into the lignin of transgenic tobacco (*Nicotiana tabacum* L.) plants with reduced expression of cinnamyl alcohol dehydrogenase. Planta **201,** 311-318.

Wolfinger, R.D., Gibson, G., Wolfinger, E.D., Bennett, L., Hamadeh, H., Bushel, P., Afshari, C., and Paules, R.S. (2001). Assessing gene significance from cDNA microarray expression data via mixed models. J. Comput. Biol. **8,** 625-637.

Xu, F., Sun, R.-C., Sun, J.-X., Liu, C.-F., He, B.-H., and Fan, J.S. (2005). Determination of cell wall ferulic and *p*-coumaric acids in sugarcane bagasse. Anal. Chim. Acta **552,** 207-217.

Zhong, R., Morrison III, W.H., Himmelsbach, D.S., Poole II, F.L., and Ye, Z.-H. (2000). Essential role of caffeoyl coenzyme A *O*-methyltransferase in lignin biosynthesis in woody poplar plants. Plant Physiol. **124,** 563-577.